PHYSICAL REVIEW E **81**, 040301(R) (2010)

Diffusion and velocity autocorrelation at the jamming transition

Peter Olsson
Department of Physics, Umeå University, 901 87 Umeå, Sweden

(Received 13 October 2009; revised manuscript received 19 February 2010; published 14 April 2010)

We perform numerical simulations to examine particle diffusion at steady shear in a soft-disk model in two dimensions and zero temperature around the jamming density. We find that the diffusion constant depends on shear rate as $D \sim \dot{\gamma}$ below jamming and as $D \sim \dot{\gamma}^{q_D}$ with $q_D < 1$ at the transition and set out to relate this to properties of the velocity autocorrelation function. It is found that this correlation function is governed by two processes with different time scales. The first time scale, the inverse of the externally applied shear rate, controls an exponential decay of the correlations whereas the second time scale, equal to the inverse shear stress, governs an algebraic decay with time. The obtained value of q_D is related to these properties of the correlation function.

DOI: 10.1103/PhysRevE.81.040301 PACS number(s): 45.70.−n, 64.60.−i

As the volume fraction increases in zero-temperature collections of spherical particles with repulsive contact interaction, there is a transition from a liquid to an amorphous solid state—the jamming transition. It has been suggested that this transition is a critical phenomenon with universal critical exponents [1] and the properties of this transition continues to be a very active field of research. Simulations at steady shearing have provided strong evidence that the behavior at the jamming density actually is a critical phenomenon [2,3], but questions still remain as to what extent results and ideas from ordinary critical phenomena may be taken over to the study of jamming, as well as the fundamental reason for the observed critical behavior.

The critical behavior at jamming has so far mostly been examined through scaling analyses of time-independent quantities. A second window into the questions behind jamming is given by also examining the time dependence. One commonly expects that the time dependence should be determined by a single time scale. In supercooled liquids this time scale is readily identified as the time for escape of the particles from the cages made up of their neighbors and it is this time scale that determines key properties of supercooled liquids like viscosity and diffusion constant.

At zero temperature there is no thermally activated motion and one then has to study the system driven out of equilibrium, e.g., by imposing a shear flow with a certain shear rate $\dot{\gamma}$. One then expects that the associated time scale $1/\dot{\gamma}$ should have a role similar to the escape time in supercooled liquids and the diffusion would then be $D \sim \dot{\gamma}$. Consequently, the mean-square displacement depends only on the total shear $t\dot{\gamma}=\gamma$. An alternative view is that a higher shear rate means that the system will not have time to move to a new local minimum before it disappears due to the shearing [4] and this kinds of reasoning leads to the expectation that the distance moved per unit strain should decrease with increasing shear rate, i.e., $D \sim \dot{\gamma}^{q_D}$ with $q_D < 1$. Experiments also give conflicting results. Whereas some recent experiments on colloidal systems give $q_D = 0.80 \pm 0.01$ [5] others report a linear behavior, $q_D = 1$ [6].

In this Rapid Communication we perform shearing simulations of a simple soft-disk model in two dimensions at zero temperature to determine the diffusion constant at several densities around ϕ_J. In the region *below jamming* we confirm the expected behavior $D \sim \dot{\gamma}$, but we also find that the behavior *at the transition* is very different: $D \sim \dot{\gamma}^{q_D}$ with $q_D \approx 0.78(2)$. We furthermore find that it is possible to do a scaling collapse of D in a region around the transition. To better understand this behavior we turn to the velocity correlation function (VCF) and find that it is governed by two different time scales. Beside $1/\dot{\gamma}$ from the externally imposed shear rate, the system is also controlled by the time scale from the inverse shear stress, which we believe is related to the internal relaxation. This internal relaxation contributes with an algebraic decay to the VCF. It is found that these features together lead to an effective time scale $\tau \sim \dot{\gamma}^{-q_D}$ that controls the macroscopic behavior, as, e.g., seen through the diffusion.

Following O'Hern *et al.* [7] we simulate frictionless soft disks in two dimensions using a bidispersive mixture with equal numbers of disks with two different radii of ratio 1.4. Length is measured in units of the diameter of the small particles ($d_s = 1$). With r_{ij} for the distance between the centers of two particles and d_{ij} the sum of their radii, the interaction between overlapping particles is

$$V(r_{ij}) = \begin{cases} \dfrac{\epsilon}{2}(1 - r_{ij}/d_{ij})^2, & r_{ij} < d_{ij} \\ 0, & r_{ij} \geq d_{ij} \end{cases}.$$

We use Lees-Edwards boundary conditions [8] to introduce a time-dependent shear strain $\gamma = t\dot{\gamma}$. With periodic boundary conditions on the coordinates x_i and y_i in an $L \times L$ system, the position of particle i in a box with strain γ is defined as $\mathbf{r}_i = (x_i + \gamma y_i, y_i)$. We simulate overdamped dynamics at zero temperature with the equation of motion [9],

$$\frac{d\mathbf{r}_i}{dt} = -C \sum_j \frac{dV(\mathbf{r}_{ij})}{d\mathbf{r}_i} + y_i \dot{\gamma} \hat{x},$$

with $\epsilon = 1$ and $C = 1$. The unit of time is $\tau_0 = d_s / C\epsilon$. We integrate the equations of motion with the Heuns method, using a time step $\Delta t = 0.2\tau_0$. As this must be considered rather large, we have checked carefully that simulations with half that time step gives the same results to a very high accuracy.

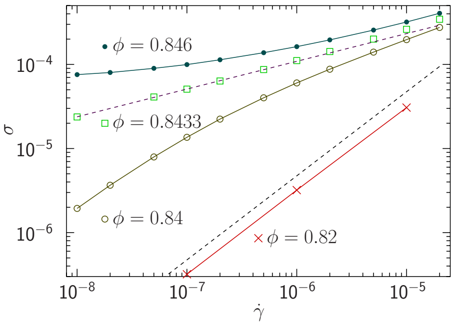

FIG. 1. (Color online) Shear stress versus shear rate around ϕ_J. Well below ϕ_J, exemplified by ϕ=0.82, we find $\sigma \propto \dot{\gamma}$. On this log-log plot that is shown by a straight line with slope=1 (lower dashed line). At ϕ=0.8433$\approx\phi_J$ the relation is algebraic, $\sigma \sim \dot{\gamma}^{q_\sigma}$, with q_σ=0.33 (upper dashed line). Data at slightly higher and lower densities (filled and open circles, respectively) show clear curvatures. In the $\dot{\gamma}\to 0$ limit they cross over to σ=const and $\sigma \propto \dot{\gamma}$, respectively.

The possibility to use such large time steps is linked to the simple dynamics, zero temperature, and our low shear rates.

The behavior of the shear stress at a few different densities at and around ϕ=0.8433$\approx\phi_J$ [10] is shown in Fig. 1. The simulations are done with N=65 536 particles except when otherwise noted. At low densities (crosses, ϕ=0.82) the shear stress is simply proportional to $\dot{\gamma}$. At $\phi \approx \phi_J$, the shear stress is algebraic in the shear rate, $\sigma \sim \dot{\gamma}^{q_\sigma}$ with q_σ =0.33, whereas the data obtained at ϕ slightly away from ϕ_J have clear curvatures. In the notation of Ref. [2], $q_\sigma=\Delta/(\beta+\Delta)$. We remark that the fit at ϕ_J is not entirely perfect. This is due to some corrections to scaling that complicate the scaling analyses and is also the reason for the somewhat different values of ϕ_J and the exponents here compared to Ref. [2].

To determine the diffusion constant, we consider the transverse displacements, i.e., the displacements in the y direction. We will related this to the VCF from the y component of the velocity,

$$g_v(t) = \langle v_y(t')v_y(t'+t)\rangle,$$

where the average is over all particles and a large number of initial times, t'. Here and in the following, t is the difference between two absolute times. The VCF has been examined before [11] but the present data with higher precision at lower shear rates make it possible to do a more thorough analysis of its properties. The relation to the diffusion constant is given by the fundamental relation

$$D = \int_{-\infty}^{\infty} dt g_v(t) = g_v(0)\int_{-\infty}^{\infty} dt G_v(t), \qquad (1)$$

where we introduce the normalized $G_v(t)=g_v(t)/g_v(0)$. It is convenient to write the expression in terms of $G_v(t)$ since the prefactor, $g_v(0)$, has a known behavior, $g_v(0)\equiv\langle v_y^2\rangle \sim \sigma\dot{\gamma}$, which follows from $N\langle \mathbf{v}^2\rangle/C=L^2\sigma\dot{\gamma}$ [11].

Our determination of the diffusion constant is illustrated in Fig. 2(a). As the figure shows it is difficult to determine D from the long time limit of $\langle\Delta y^2\rangle/t$ since this quantity approaches the constant value=D very slowly. The reason for this is a remainder of the short time behavior. For $t>t_0$, where t_0 is the range of the velocity correlations [such that $G_v(t)$ may be neglected for $t \gtrsim t_0$; we choose γ_0=0.5, $t_0 = \gamma_0/\dot{\gamma}$, cf. Fig. 3], it is easy to show that the expression for the mean-square distance is

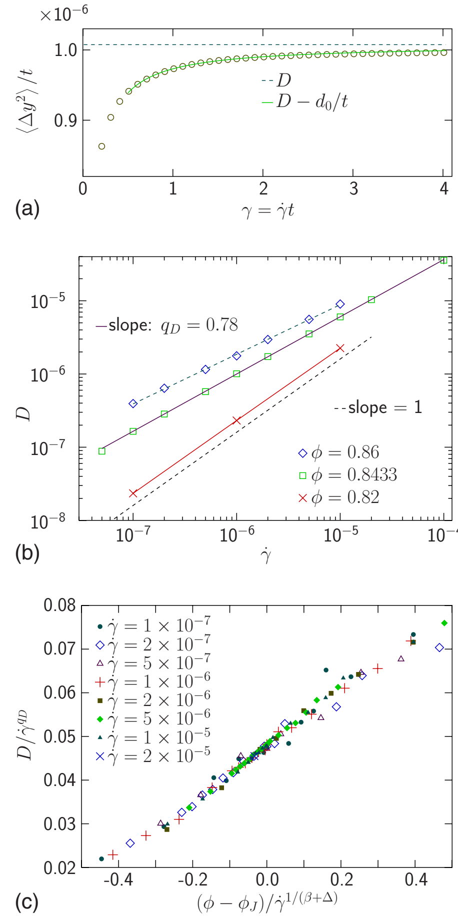

FIG. 2. (Color online) Diffusion constant around ϕ_J. Panel (a) shows the determination of D from the large γ part of data from $\dot{\gamma}$=10^{-6} and ϕ=0.8433. The solid line is from fitting $\langle\Delta y^2\rangle$ to Eq. (2). The dashed line corresponds to D. Panel (b) shows the expected behavior below jamming, $D\sim\dot{\gamma}$, together with the same data at jamming, $D\sim\dot{\gamma}^{q_D}$, with q_D=0.78(2). This slope continues to decrease with increasing ϕ and is $\approx$0.68 at ϕ=0.86. Panel (c) is a scaling collapse of the diffusion constant with q_D=0.78.

$$\langle\Delta y^2(t)\rangle = \int_0^t dt' \int_0^t dt'' g_v(t'-t'') = Dt - d_0 \qquad (2)$$

with D from Eq. (1) and $d_0=\int_0^{t_0}dt'\int_{t'}^{t_0}dt'' g_v(t'')$. The solid line in Fig. 2(a) is from a fit to Eq. (2) with data from the interval γ_0=0.5$\leq\gamma\leq$2. The dashed line is the estimated value of D.

Figure 2(b) shows diffusion constant versus shear rate at three different densities, ϕ=0.82, ϕ=0.8433$\approx\phi_J$, and ϕ =0.86. Below ϕ_J the behavior is linear and at ϕ_J the relation is algebraic, $D\sim\dot{\gamma}^{q_D}$, with q_D=0.78(2). This slope continues to decrease as ϕ increases above ϕ_J and is $\approx$0.68 at ϕ =0.86. Using q_D=0.78 together with $1/(\beta+\Delta)$=0.275 from

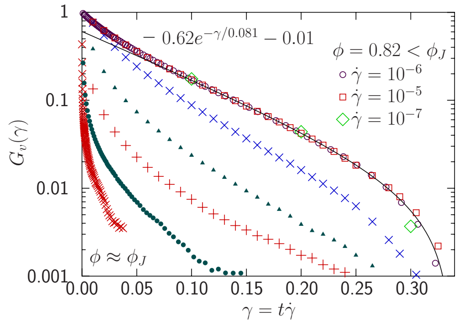

FIG. 3. (Color online) Scaling properties of the VCF below and at ϕ_J. The collapse of $G_v(\gamma)$ at ϕ=0.82 (upper points) nicely shows that the behavior is governed by γ, which implies that $1/\dot\gamma$ is the relevant time scale. The lower points which show $G_v(\gamma)$ at ϕ_J clearly fail to scale. The solid line shows that G_v decays exponentially, $e^{-\gamma/\gamma_1}$ with γ_1=0.081 down to a negative value. The meaning of the symbols for the data at $\phi \approx \phi_J$ is given in Fig. 4(a).

a scaling analysis of the energy to be discussed elsewhere, it is possible to collapse D in a region around ϕ_J as shown in Fig. 2(c).

To search for a reason for this nontrivial behavior we turn to the VCF. Figure 3 shows very clearly that the behaviors below ϕ_J and at ϕ_J, respectively, are very different. At $\phi = 0.82 < \phi_J$ the VCF collapses when plotted against γ whereas the same data at $\phi \approx \phi_J$ fails badly to collapse. The low-density data decay exponentially $\sim e^{-\gamma/\gamma_1}$ with $\gamma_1 \approx 0.081$ to a negative value ≈ -0.01 as shown by the solid line. Such nonmonotonic behavior with a dip below zero [11] is familiar from liquids in equilibrium [12].

The dramatic failure to collapse is at first difficult to reconcile with the value $q_D \approx 0.78(2)$ which is not very far from unity. It is therefore interesting to ask what scaling we should expect for $G_v(t;\dot\gamma)$ to give $q_D=1$ at ϕ_J. Considering the prefactor of Eq. (1), $g_v(0) \sim \dot\gamma\sigma$, it follows that $q_D=1$ only if $\int dt G_v(t;\dot\gamma)=1/\sigma$, which suggests the scaling $G_v(t;\dot\gamma) = \tilde{G}(t\sigma)$. To check this we plot $G_v(t)$ at ϕ_J against $t\sigma$ for several different shear rates in Fig. 4(a). Just as expected (since $q_D \neq 1$) there is no perfect collapse of the data, but it is interesting to note that the data agree reasonably well at small times. Figure 4(b) is the same kind of plot but only including data for small total shear, $\gamma < 0.01$. These data collapse nicely and actually suggests an algebraic scaling function, $\tilde{G}(x) \sim x^{-\lambda}$, for $x > 0.5$, where λ is a new fundamental exponent.

It turns out that the deviations from a common curve in Fig. 4(a) may be ascribed to an exponential decay and that the VCF may be written $G_v(t;\dot\gamma) = \tilde{G}(t\sigma)e^{-\gamma/\gamma_1}$. Figure 4(c) shows $\tilde{G}(t\sigma)$ obtained by choosing $\gamma_1=0.081$, (the same as in the exponential decay of the low-density data in Fig. 3). The collapse is very good and the scaling function is clearly algebraic. The slope in Fig. 4(c) gives $\lambda = 0.77(2)$.

From these findings we conclude that the behavior is controlled by two time scales and their associated processes. Beside the externally given time scale $t_1 = \gamma_1/\dot\gamma$ that controls an exponential decay of $G_v(t)$ there is a time scale from the inverse shear stress $t_{\mathrm{int}} = 1/C\sigma$, which governs an algebraic decay. We believe that this is the time scale that controls the

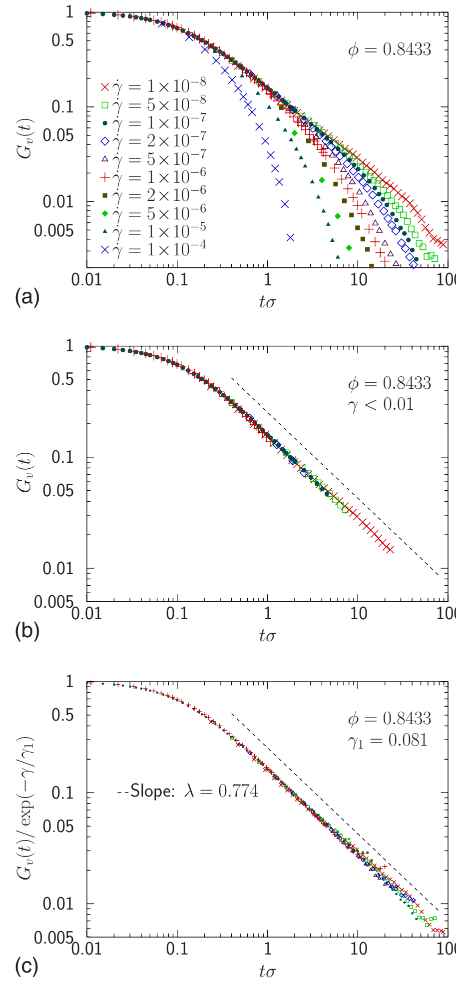

FIG. 4. (Color online) Attempted scaling collapse of the VCF at ϕ_J. Panel (a) shows a failure to collapse, except at very short times. It is then seen in panel (b) that the data for a small total shear, $\gamma < 0.01$, actually collapse nicely and that the behavior at large times is algebraic. Finally, panel (c) shows that it is possible to make all data with $\dot\gamma \geq 10^{-5}$ collapse by compensating for the exponential decay, $e^{-\gamma/\gamma_1}$, with γ_1=0.081. The simulation for the lowest shear rate was here done with twice as many particles (N=131 072) to avoid finite-size effects that become visible in $G_v(t)$ before they are seen in most other quantities.

internal relaxation of plastic events [4]. Below jamming where $\sigma \propto \dot\gamma$ one has $t_{\mathrm{int}} \propto t_1$ and there is in effect only a single time scale.

The focus of the present investigation is a comparison of the transport properties at and below the jamming transition, respectively. It should nevertheless be mentioned that the functional form of G_v above ϕ_J appears to be rather similar with both algebraic and exponential behaviors. The detailed study of this is however complicated by the finite-size effects [13] that are expected at higher densities and is left to future work.

We now want to express q_D in terms of the exponents q_σ and λ that characterize the scaling of $G_v(t;\dot\gamma)$. The simplest approximation is to neglect the saturation of G_v at small t and, in effect, assume that $G_v(t;\dot\gamma) \propto (t\dot\gamma^{q_\sigma})^{-\lambda} e^{-t\dot\gamma/\gamma_1}$ holds down to t=0. This should be an excellent approximation in the limit of small $\dot{\gamma}$. From Eq. (1) and $g_v(0)\sim\dot{\gamma}^{1+q_\sigma}$ we get

$$D\sim\dot{\gamma}^{1+q_\sigma}\dot{\gamma}^{-q_\sigma\lambda}\left(\frac{\dot{\gamma}}{\gamma_1}\right)^{\lambda-1}\int_0^\infty dx x^{-\lambda}e^{-x}\sim\dot{\gamma}^{\lambda+(1-\lambda)q_\sigma},$$

and obtain $q_D^0=\lambda+(1-\lambda)q_\sigma=0.85(3)$ as the estimate of this exponent in the $\dot{\gamma}\to 0$ limit. Note that this result is dominated by the first term; the value of q_D^0 is mostly controlled by λ. It is also interesting to note that this expression gives $q_D=1$ if $q_\sigma=1$; i.e., $\sigma\propto\dot{\gamma}$ implies that $D\sim\dot{\gamma}$.

Including the saturation of G_v at small t in the integration above adds a term proportional to $\dot{\gamma}$ to the expression for D. The effect of this term will be perceived as a lower effective value of q_D at the shear rates accessible in the simulations. Note that this is consistent with $q_D=0.78(2)$ from Fig. 2(b) being slightly lower than the numerical value $q_D^0=0.85(3)$, though the differences are not much bigger than the expected statistical uncertainties.

An interesting finding in the above analysis is the algebraic behavior of the correlations at large t and small γ shown in Fig. 4. Algebraic decay of velocity correlations have been found before [14] in molecular-dynamics simulations, but since that effect is attributed to the conservation (and decay) of momentum, that kind of mechanism cannot be relevant here in this model with no inertia. We instead speculate that the algebraic behavior is related to the finding from quasistatic simulations that individual plastic events often are avalanches of elementary flips [13,15–17] and that these avalanches have the effect to increase the diffusion and therefore also to increase the VCF. Another reason for making this connection is ideas from self-organized criticality—with the paradigmatic sandpile model—that a slowly driven system can automatically adjust itself such that there are avalanches on all length and time scales, which would be seen through power laws in various quantities.

To conclude, we have found that the relation between diffusion and shear rate is very different below ϕ_J and at ϕ_J, respectively, and that this difference is related to two time scales that happen to be proportional to one another below ϕ_J but become very different at ϕ_J. These time scales are $t_1=\gamma_1/\dot{\gamma}$ from the externally applied shear rate and $t_{\rm int}=1/(C\sigma)\sim\dot{\gamma}^{-q_\sigma}$ that controls the internal relaxation. The normalized VCF is $G_v(t;\dot{\gamma})=\tilde{G}(t/t_{\rm int})e^{-t/t_1}$, where $\tilde{G}(x)\sim x^{-\lambda}$ for large x and λ is a new fundamental exponent. These two fundamental time scales and the exponent λ together lead to an effective time scale $\tau\sim\dot{\gamma}^{-q_D}$ that controls the macroscopic behavior as seen through the diffusion constant. We also speculate that the algebraic decay seen in the relaxational part of the dynamics is related to avalanches of elementary flips and could be a manifestation of self-organized criticality.

I thank P. Minnhagen and S. Teitel for helpful discussions. This work was supported by the Swedish Research Council and the High Performance Computer Center North.

[1] A. J. Liu and S. R. Nagel, Nature (London) **396**, 21 (1998).
[2] P. Olsson and S. Teitel, Phys. Rev. Lett. **99**, 178001 (2007).
[3] T. Hatano, J. Phys. Soc. Jpn. **77**, 123002 (2008).
[4] D. L. Malandro and D. J. Lacks, Phys. Rev. Lett. **81**, 5576 (1998).
[5] R. Besseling, E. R. Weeks, A. B. Schofield, and W. C. K. Poon, Phys. Rev. Lett. **99**, 028301 (2007).
[6] C. Eisenmann, C. Kim, J. Mattsson, and D. A. Weitz, Phys. Rev. Lett. **104**, 035502 (2010).
[7] C. S. O'Hern, L. E. Silbert, A. J. Liu, and S. R. Nagel, Phys. Rev. E **68**, 011306 (2003).
[8] D. J. Evans and G. P. Morriss, *Statistical Mechanics of Nonequilibrium Liquids* (Academic, London, 1990).
[9] D. J. Durian, Phys. Rev. Lett. **75**, 4780 (1995).
[10] C. Heussinger and J.-L. Barrat, Phys. Rev. Lett. **102**, 218303 (2009).
[11] I. K. Ono, S. Tewari, S. A. Langer, and A. J. Liu, Phys. Rev. E **67**, 061503 (2003).
[12] J. E. Variyar, D. Kivelson, G. Tarjus, and J. Talbot, J. Chem. Phys. **96**, 593 (1992).
[13] A. Lemaître and C. Caroli, Phys. Rev. Lett. **103**, 065501 (2009).
[14] B. J. Alder and T. E. Wainwright, Phys. Rev. A **1**, 18 (1970).
[15] C. E. Maloney and A. Lemaître, Phys. Rev. E **74**, 016118 (2006).
[16] J. Goyon, A. Colin, G. Ovarlez, A. Ajdari, and L. Bocquet, Nature (London) **454**, 84 (2008).
[17] E. Lerner and I. Procaccia, Phys. Rev. E **79**, 066109 (2009).